

2

WRDC-TR-89-4063



NOV 11 1989

**INTERFACES OF ORGANIC MATRICES AND  
GRAPHITE FIBER COMPOSITES:  
A REVIEW OF THE LITERATURE**

Karla L. Strong, 1Lt  
Structural Materials Branch  
Nonmetallic Materials Division

8 July 1989

Final Report for Period Aug 88-May 89

Approved for public release; distribution unlimited

DTIC  
ELECTE  
NOV 03 1989  
S B D  
Co

MATERIALS LABORATORY  
WRIGHT RESEARCH DEVELOPMENT CENTER  
AIR FORCE SYSTEMS COMMAND  
WRIGHT-PATTERSON AIR FORCE BASE, OHIO 45433-6533

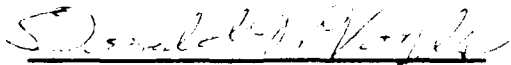
AD-A214 504

NOV 11 1989

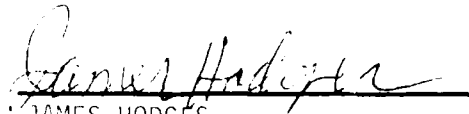
## NOTICE

WHEN GOVERNMENT DRAWINGS, SPECIFICATIONS, OR OTHER DATA ARE USED FOR ANY PURPOSE OTHER THAN IN CONNECTION WITH A DEFINITELY GOVERNMENT-RELATED PROCUREMENT, THE UNITED STATES GOVERNMENT INCURS NO RESPONSIBILITY OR ANY OBLIGATION WHATSOEVER. THE FACT THAT THE GOVERNMENT MAY HAVE FORMULATED OR IN ANY WAY SUPPLIED THE SAID DRAWINGS, SPECIFICATIONS, OR OTHER DATA, IS NOT TO BE REGARDED BY IMPLICATION, OR OTHERWISE IN ANY MANNER CONSTRUED, AS LICENSING THE HOLDER, OR ANY OTHER PERSON OR CORPORATION; OR AS CONVEYING ANY RIGHTS OR PERMISSION TO MANUFACTURE, USE, OR SELL ANY PATENTED INVENTION THAT MAY IN ANY WAY BE RELATED THERETO.

THIS TECHNICAL REPORT HAS BEEN REVIEWED AND IS APPROVED FOR PUBLICATION.

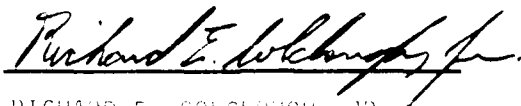


DONALD W. VOYLS, Program Manager  
Aircraft Battle Damage Repair  
Advanced Development Technology



JAMES HODGES  
Survivability Enhancement Branch  
Vehicle Equipment Division

FOR THE COMMANDER



RICHARD E. COLCLOUGH, JR.  
Chief  
Vehicle Equipment Division

IF YOUR ADDRESS HAS CHANGED, IF YOU WISH TO BE REMOVED FROM OUR MAILING LIST, OR IF THE ADDRESSEE IS NO LONGER EMPLOYED BY YOUR ORGANIZATION PLEASE NOTIFY WPD/VE150, WRIGHT PATTERSON AFB, OH 45433 5053 TO HELP MAINTAIN A CURRENT MAILING LIST.

COPIES OF THIS REPORT SHOULD NOT BE RETURNED UNLESS RETURN IS REQUIRED BY SECURITY CONSIDERATIONS CONTRACTUAL OBLIGATIONS, OR NOTICE ON A SPECIFIC DOCUMENT

REPORT DOCUMENTATION PAGE				Form Approved OMB No. 0704-0188		
1a. REPORT SECURITY CLASSIFICATION UNCLASSIFIED			1b. RESTRICTIVE MARKINGS			
2a. SECURITY CLASSIFICATION AUTHORITY			3 DISTRIBUTION/AVAILABILITY OF REPORT Approved for Public Release; Distribution is Unlimited.			
2b. DECLASSIFICATION/DOWNGRADING SCHEDULE						
4. PERFORMING ORGANIZATION REPORT NUMBER(S)  WRDC-TR-89-4063			5 MONITORING ORGANIZATION REPORT NUMBER(S)			
6a. NAME OF PERFORMING ORGANIZATION Wright Research & Development Ctr Structural Materials Branch Nonmetallic Materials Division		6b. OFFICE SYMBOL (If applicable)  WRDC/MLBC	7a. NAME OF MONITORING ORGANIZATION			
6c. ADDRESS (City, State, and ZIP Code)  WRDC/MLBC Wright-Patterson AFB, OH 45433-6533			7b. ADDRESS (City, State, and ZIP Code)			
8a. NAME OF FUNDING / SPONSORING ORGANIZATION		8b. OFFICE SYMBOL (If applicable)	9 PROCUREMENT INSTRUMENT IDENTIFICATION NUMBER			
8c. ADDRESS (City, State, and ZIP Code)			10 SOURCE OF FUNDING NUMBERS			
			PROGRAM ELEMENT NO  62102F	PROJECT NO.  2419	TASK NO  01	WORK UNIT ACCESSION NO  30
11. TITLE (Include Security Classification)  Interfaces of Organic Matrices and Graphite Fiber Composites: A Review of the Literature						
12 PERSONAL AUTHOR(S) Karla L. Strong						
13a. TYPE OF REPORT Final		13b. TIME COVERED FROM Aug 88 TO May 89		14. DATE OF REPORT (Year, Month, Day) July 1989		15 PAGE COUNT 47
16. SUPPLEMENTARY NOTATION						
17. COSATI CODES			18. SUBJECT TERMS (Continue on reverse if necessary and identify by block number)			
FIELD	GROUP	SUB-GROUP	Organic Matrix Composites, Graphite Fiber Composites, Composite Interface, Composite Interphase, Surface Properties of Graphite Fibers			
19. ABSTRACT (Continue on reverse if necessary and identify by block number) One of the most interesting and unique problems with advanced organic matrix composites is the fiber/matrix interface (or interphase), which is crucial in determining the material's overall properties. In the past, adhesion between the fiber and matrix has been induced by trial and error. With the current explosion of material systems and the advent of inert thermoplastic matrix materials, much more energy from industry and academia has gone into investigating and defining the interface, yet real scientific understanding eludes them.  This report reviews the current literature concerning the interface between the organic matrix materials and graphite fibers. Concepts introduced include wetting, adhesion, fiber surface modification, methods of investigation of fibers and matrices, surface chemistry, and morphology of graphite fibers and organic matrix materials. In addition, the interfacial effort on mechanical properties and interfacial shear strength testing are reviewed. It is determined that a complete scientific understanding of the chemistry, morphology, electrostatic nature, and molecular conformation of the carbon fiber surface and matrix materials is essential to alleviate poor adhesion in organic matrix composites. References included.						
20 DISTRIBUTION/AVAILABILITY OF ABSTRACT <input checked="" type="checkbox"/> UNCLASSIFIED/UNLIMITED <input type="checkbox"/> SAME AS RPT <input type="checkbox"/> DTIC USERS			21 ABSTRACT SECURITY CLASSIFICATION UNCLASSIFIED			
22a NAME OF RESPONSIBLE INDIVIDUAL 1Lt Karla L. Strong			22b TELEPHONE (Include Area Code) (513) 255-3104		22c OFFICE SYMBOL WRDC/MLBC	

## Acknowledgment

I wish to thank Dr. Ronald Allred for his review and encouragement in publication of this manuscript, and Mr. Tobey Cordell for motivating me to collect all this data into one document.

201101

Accession For	
NTIS	<input checked="checked" type="checkbox"/>
DTIC	<input type="checkbox"/>
Unannounced	<input type="checkbox"/>
Justification	
By	
Distribution/	
Availability	
Dist	Special
A-1	

## Contents

	Page
Acknowledgment . . . . .	iv
Figures . . . . .	vi
Tables . . . . .	vii
1. Introduction . . . . .	1
2. Adhesion . . . . .	2
2.1 Surface Interactions . . . . .	2
2.2 Adhesion Mechanisms . . . . .	4
2.3 Fiber Surface Modifications . . . . .	6
3. Constituents . . . . .	7
3.1 Graphite Fiber . . . . .	7
3.2 Matrix Polymers . . . . .	14
4. Interface . . . . .	18
4.1 Observation of the Interface . . . . .	18
4.2 Interface Impact on Composite Properties . . . . .	23
5. Interfacial Shear Strength Tests . . . . .	27
5.1 Single Fiber Pull-out Tests . . . . .	27
5.2 Embedded Interfacial Shear Method . . . . .	28
5.3 Microdebond Test . . . . .	35
6. Summary and Conclusions . . . . .	37
References . . . . .	39

## Figures

	Page
Figure 1. Geometry of test measuring liquid contact angle . . . . .	3
Figure 2. Adhesion mechanisms . . . . .	4
Figure 3. A schematic representation of the structure of carbon fibers based on X-ray diffraction and electron microscopy. . . . .	9
Figure 4. The bombardment of an atom with X-rays. . . . .	10
Figure 5. Spectra of carbon fibers at various carbonization temperatures . . . . .	11
Figure 6. Schematic structure of the model interface . . . . .	13
Figure 7. Reactions between epoxy resins and hardeners and carbon fiber surface groups . . . . .	14
Figure 8. Some thermoplastic structural formulas . . . . .	15
Figure 9. Photograph of transcrystallinity in PEEK . . . . .	16
Figure 10. SEM photomicrographs of composite fracture surfaces . . . . .	19-20
Figure 11. SEM photomicrograph of etched cross section of APC-2 laminate cooled at 15°C/min . . . . .	21
Figure 12. Interface impact on composite properties . . . . .	24
Figure 13. Schematic of single fiber pull-out method . . . . .	28
Figure 14. Schematics of embedded interfacial shear and microdebond methods . . . . .	29
Figure 15. Geometry of embedded interfacial shear test specimen . . . . .	30
Figure 16. Birefringence in well-bonded XAS fiber in polycarbonate . . . . .	30
Figure 17. Schematic of tensile and shear stress concentrations at the fiber ends . . . . .	32

## Tables

	Page
Table 1 XPS analysis of graphite fiber surface chemistry . . . . .	12
Table 2 XPS analysis of fiber surface after treatment . . . . .	12
Table 3 Transcrystallinity and mechanical properties . . . . .	22
Table 4 Variation in mechanical properties with fiber surface treatment and sizing . . . . .	25
Table 5 IFSS of PAN and pitch-based fibers in DER#331 . . . . .	32
Table 6 IFSS of PAN-based fibers in thermoplastic matrices . . . . .	33
Table 7 IFSS variation with surface treatment . . . . .	34
Table 8 Microdebond testing of thermoplastic matrix composites . . . . .	36

# **Interfaces of Organic Matrices and Graphite Fiber Composites: A Review of the Literature**

## **1. Introduction**

In the last 20 years, a new category of engineering materials has arisen--advanced composites. These materials are stronger and lighter than earlier structural materials, and their properties are tailorable to specific applications. They are ideally suited to the aerospace industry to achieve increased performance and fuel cost savings. Since they are new materials, less is known about them than conventional materials. This information must be discovered before advanced composites are widely accepted.

One of the more interesting and unique problems with advanced composites is the fiber/matrix interface. The area where two materials come into intimate contact is crucial in the material's overall properties. In the past, adhesion has been generated by trial and error. This method has been sufficient while the number of distinct systems was relatively small and the matrix and fiber inherently compatible. However, with the current explosion of material systems and the advent of inert thermoplastic matrix materials, much more energy from industry and academia has gone into investigating and defining the interface. More and more it is clear that a complete scientific understanding of the chemistry, morphology, electrostatic nature, and molecular conformation of the carbon fiber surface and various matrix materials is essential to alleviate poor adhesion in organic matrix composites.

In this report, the concepts of wetting and adhesion are first clarified, then methods of fiber surface modification are explained. Next, the chemistry and morphology of graphite fibers and organic matrix materials are examined, and experimentation methods of fibers and matrices are elaborated. Then the nature of the interface itself is established. Finally, mechanical properties and interfacial shear strength testing are reviewed.



achieve the best possible interface and, (b) wetting is a function of the surface free energies of the polymer and the energy of the liquid/fiber surface.

Berger claims that Lewis acid and base interactions significantly effect wetting. Lewis acids are electron accepters and Lewis bases are electron donors. Wetting studies can be conducted in which the fiber is immersed into the liquid and the force of immersion or emmersion is measured. From that, the contact angle can be calculated. Figure 1 shows the geometry of this test. Using basic and acidic liquids to perform the test, we can determine whether the fiber surface is a Lewis acid or base. Acidic fibers are wet better with basic liquids. Also, slightly acidic liquids wet a slightly basic fiber surface better than a strongly acidic liquid could, and vice-versa. It has been discovered that water-sized glass fibers are basic, and epoxy-sized glass and polyarimid fibers are slightly acidic. Knowing this, a resin of opposite pKa is a better choice for wetting purposes (3).

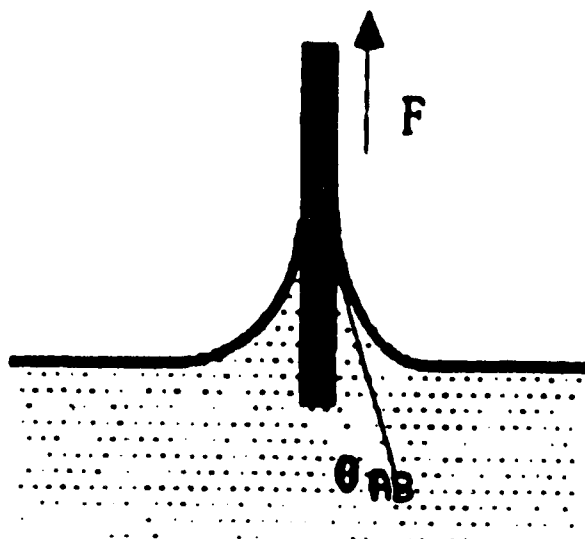


Figure 1. Geometry of test measuring liquid contact angle (4)

There are various approaches to improve wetting. First, decreasing viscosity by increasing pressure, contact time, or temperature during processing will help. Also, removing the outer layers of adsorbed gasses on the fiber or increasing the surface roughness of the fiber may change the surface free energy. Finally, changing the chemistry of the fiber surface or that of the resin may alter the surface free energy to drive the fiber and matrix to join. In practice, all of these methods are used to some degree. Some of the processes which may improve wetting are reviewed later in this report.

## 2.2 Adhesion Mechanisms

There are several ways in which fibers and matrix materials can "stick" to each other. They are shown schematically in Figure 2.

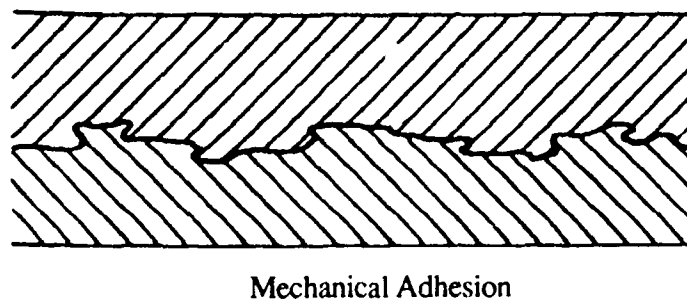
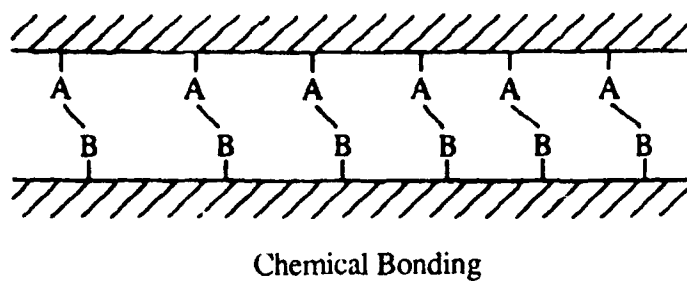
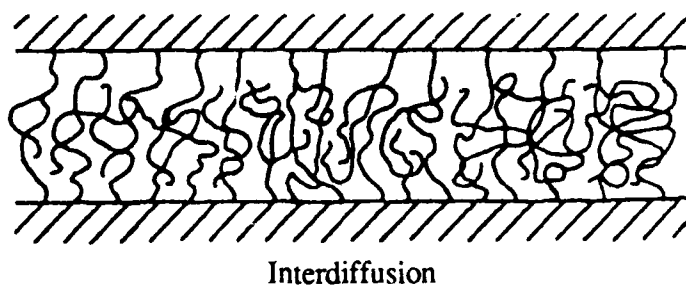
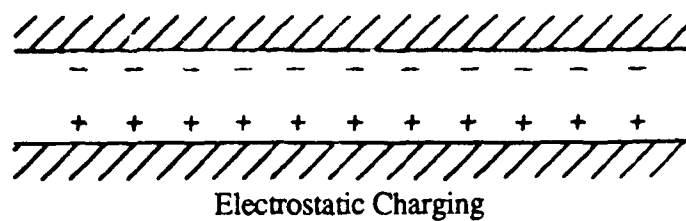


Figure 2. Adhesion mechanisms

### *2.2.1 Interdiffusion*

The long polymer molecules of the matrix may intertwine with long molecules attached to the fiber surface. These polymers can be attached to the fiber by electrostatic charging or chemical bonding. In one study, Allen Crasto and his colleges have used carbon fibers as electrodes to form polymer coating or *size* on the fiber via electrodeposition of an ethylene acrylic acid random copolymer (EAA). They found that both the interfacial shear strength (IFSS) and the impact strengths of the composites made with these fibers were improved. The increase in IFSS is easily explained by thinking that the matrix material (EPON 828 with m-PDA) was able to intertwine with the size to create strong adhesion. In addition, the EAA was suspected to increase the surface energy of the fiber for better wetting. The impact strength was improved because the interphase acted as a deformable layer that absorbed energy by blunting and deflecting the crack tip as it propagated (5). From these results, it is apparent that the intertwining method may be one system to increase adhesion with thermoplastic composites.

### *2.2.2 Electrostatic Charging*

If the matrix has one charge and the fiber the opposite, electrostatic forces will hold the materials together. This category includes Lewis acid and base interactions such as hydrogen bonding. English researchers of fiber/matrix interactions, Denison and Jones, have shown that carbon fiber surface carboxylic acid groups coordinate with the amine hardener in epoxies by hydrogen bonding (6).

### *2.2.3 Chemical Bonding*

Covalent bonds are the strongest method of fiber/matrix adhesion. Sites on the carbon fiber can react during processing to create an actual chemical link between the fiber and the matrix. This is very common between glass fibers and epoxy matrices where an organic silane coating is deposited on the glass fibers before processing. The size polymerizes in the presence of water (which is common on glass fibers) to create a polysilane layer which chemically links the fiber to the matrix.

### *2.2.4 Mechanical Adhesion*

If the fibers possess ridges and other topographical variations, the liquid polymer can fill in these spaces and solidify, locking the two together mechanically (7). In fact, Harvey, et al. have found that interlaminar shear strength (ILSS) is not just a function of the surface oxygen and conclude that mechanical keying of the resin to the fiber surface is likely to play a more important role in adhesion than many other workers believe (8).

### 2.3 Fiber Surface Modifications

Sizings and surface treatments are the dominant ways to modify carbon fiber surface reactivity. Sizings are simply coatings deposited on the fiber, usually very soon after its manufacture. Most often, sizings are meant to improve handlability of the fiber during weaving and prepregging, or to protect the fiber from damage or chemical attack. The sizing must be compatible with the matrix material to allow some adhesion, but often sizings are chemically designed to promote adhesion.

There are several different ways to surface treat a fiber, but most are methods by which oxygen functionality is added to the fiber surface. Oxidative acid baths are most common, but plasmas such as oxygen, nitrogen, ammonia, and carbon dioxide have been used. The plasmas are usually excited by a radio frequency at low power. Dr. Ronald Allred of PDA Engineering has successfully used ammonia and carbon dioxide plasma treatments on graphite fibers to create covalent bonds with thermoplastic polymers. PDA carefully monitors the plasma treatments which attack graphite basal planes as well as edge sites to add radicals, peroxides, and lactones. In some cases, they believe that the graphitic plane is interrupted to create imperfections. Not only do plasma treatments change the surface reactive groups, but they also increase surface energetics. Plasma removal of the outer circumferential graphitic planes can also increase the number of reactive sites on the fiber surface. Plasma treatments can be acidic or basic to increase the likelihood of fiber wetting by the liquid resin (9).

### 3. Constituents

#### 3.1 Graphite Fibers

##### *3.1.1 Production and Properties*

Carbon or graphite fibers are made primarily from two raw materials, polyacrylonitrile (PAN) and mesophase pitch, a by-product of oil refining. PAN-based fibers are first spun, and then stretched. Stretching is used to orient the polymer along the axis of the fiber. While still under tension, the fibers are heated to "set" the orientation by reacting the active nitrile groups at elevated temperatures to produce oriented ladder polymer filaments. Further heating carbonizes and graphitizes the PAN. Pitch-based fibers are spun, orienting the pitch liquid crystals, then carbonized and graphitized under tension. Both types of fiber are carbonized at about 1,000-1,700°C and graphitized as high as 2,500-2,800°C (10). The fibers formed are turbostratic graphite--layers of graphite sheets in a random arrangement held together with weak Van der Waals forces. The layers lie along the fiber axis. They are very anisotropic; strong and stiff in the longitudinal direction, but weak in the transverse direction. Fibers are normally between 6-10 microns in diameter, with an average of about 7 microns. As the orientation of the graphitic planes increases, the modulus increases. Pitch-based fibers are generally of greater modulus than the PAN-based, and have been found to be more perfectly oriented and to have greater crystallite size. Whether basal planes or edges are exposed affects what surface chemical groups are present.

Of course, several residual artifacts from the manufacturing process affect the fiber itself. First, the morphology of the precursors is carried through to the final product. If the precursor is highly oriented along the fiber axis, the graphite planes will be also. Any defects in the precursors, such as impurities, imperfect chains or crystals, and surface features, are intact in the fiber. Surface striations which appear on the PAN precursor will be present in the final product. Unusually shaped PAN fibers can even be spun and retain their shape in the graphite fiber. This concept is being more fully explored in the USAF Ultra-lightweight program, Wright Research and Development Center, Materials Laboratory, contract numbers F33615-88-C-5452 and F66615-88-C-5447.

The strength of carbon fibers is actually a distribution of strengths which is controlled by defects in the fiber. The Weibull distribution is widely used in reliability and is applicable for reduction of data concerning the strength of carbon and graphite fibers (11).

### *3.1.2 Investigative Techniques for Graphite Fibers*

Some of the methods used to study graphite fibers are discussed below:

#### *3.1.2.1 Scanning Electron Microscopy (SEM)*

Scanning electron microscopy has a resolution of about 5 nm--small enough to observe the surface roughness of individual fibers which is important for consideration of mechanical interlocking adhesion. It can also be used to study interior morphology of fractured fibers, although the clarity of such micrographs is mediocre unless a new high-resolution microscope is used. In this machine, crystallites can be viewed individually and their relative orientations determined. Photomicrographs reveal that higher modulus fibers do have greater orientation and that the surface layers of most fibers appear to be circumferential, while the interior is less ordered.

#### *3.1.2.2 Raman Spectroscopy*

When a molecule is exposed to electromagnetic radiation, the energy can be transmitted, absorbed, or scattered. In Raman spectroscopy, the energy is scattered after the photons of energy interact with the molecule. The incident energy raises the molecule to a higher vibrational or rotational energy state, then it drops to a lower one. If it drops to a state different than that it first occupied, the Raman shift occurs. The shift is proportional to the energy differences in the vibrational and/or rotational energy levels of the molecule, which are characteristic of each type of covalent bond (e.g. C=O, benzene ring, etc.). Hence, the molecular state of the sample can be determined (12).

Raman spectroscopy discerns the surface layer only a few hundred angstroms thick, and its resolution is about 1 micron. It is ideal for studying fiber and fracture surfaces. A single crystal of graphite has a sharp peak at  $1580\text{ cm}^{-1}$ . As the imperfection of the crystal increases, a  $1,380\text{ cm}^{-1}$  band appears, the  $1,580$ -band shifts to higher wave number, a shoulder appears on the peak at about  $1,620\text{ cm}^{-1}$ , and the width of both bands increases. With the use of standards, this information can be quantified. Much information about the near-surface structure of the fiber can be gained.

One Raman study compared PAN- and pitch-based fibers. It has been observed that thermoplastics are less apt to adhere to pitch-based fibers than to PAN-based ones. These researchers concluded that pitch fibers are more graphitized at the surface than PAN fibers, just as suspected. Defects and free basal plane edges promote adhesion (13).

#### *3.1.2.3 Secondary Ion Mass Spectroscopy (SIMS)*

In SIMS, the sample is bombarded with ions, known as the primary ions, which destructively erode the sample surface. The ions that are evolved from the surface are secondary ions. Both monatomic and ionic groups are formed. These secondary ions are analyzed by mass spectroscopy. If the ion beam is in a scanning mode, the origin of the secondary ions can be

determined to give an "ion map" of the surface about 1.4 microns in diameter (14). The ions traced can be positive or negative. Positive ion analysis of carbon fibers has found traces of Li, Na, Mg, Al, Si, K, Ca, Ti, Cr, and Fe. Negative ions detected include O, N, F, S, and Cl (15). Since this is an erosive process, a depth profile can be made of the specimen. The analysis depth is about 1 to 2 nm per pass (16). The other advantage of SIMS is that it can detect hydrogen, which the other methods cannot.

SIMS has been used to analyze fibers after sizing because it can detect very thin layers of polymer deposited on the fiber that SEM could miss. Carboxylic acid groups have been detected on treated fibers (17).

#### 3.1.2.4 X-Ray Diffraction (XRD)

X-ray diffraction is explained as reflections of X-rays from a stack of crystal planes and is described by Bragg's law,  $n\lambda = 2d\sin\theta$ . XRD gives information about the graphite crystals in the bulk of the fiber. Figure 3 shows a schematic representation of the structure of carbon fibers based on X-ray diffraction and electron microscopy. Workers at Toray have studied the (002) reflection of the graphitic planes and have discovered that for PAN based fibers heat-treated at 2,500°C, the average crystallite size is about 5 nm (18). As the graphitization temperature increases, the  $2\theta$  band at about 25° narrows, indicating greater orientation of the graphitic planes. Diffraction also gives the parameters of a graphite crystal lattice.

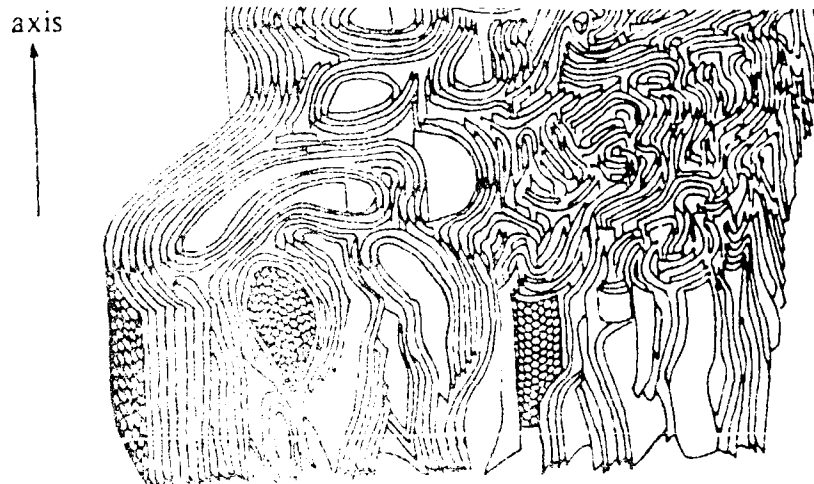


Figure 3. A schematic representation of the structure of carbon fibers based on X-ray diffraction and electron microscopy (19)

#### 3.1.2.5 Auger Electron Spectroscopy (AES)

When an atom is bombarded by X-rays, the kinetic energy can be absorbed by imparting energy to an electron, then expelling it. This process is called photoelectric absorption and the ejected electron is called a photoelectron. But then, an extra place for an electron exists in an interior shell of the atom which must be filled. If an electron from an outer shell fills the space,

then an X-ray is emitted. If, however, that X-ray is also absorbed by an electron in the same atom, that electron is also ejected. That is an Auger electron. When bombarded with monochromatic X-rays, the emitted Auger electrons create a series of peaks in a graph of the energy versus the intensity. The energy of the electrons is characteristic of the emitter for each shell, and, fortunately, only the electrons from the top several atom layers (about the first 30-40) contribute to the Auger spectrum since only they have enough energy to escape the surface of the sample. Resolution of Auger spectroscopy can be as low as 50 nm. Figure 4 shows how X-rays, photoelectrons and Auger electrons are evolved (20).

The Auger phenomenon happens more readily in low atomic number elements because the electrons are bound more loosely, making it especially useful for carbon. The sample may be scanned to obtain an image or map of the elements on the surface. For carbon fibers, AES is used for composition analysis only, because the chemical state is difficult to read as the peaks of energy intensity widen. To investigate fracture surfaces or composites in situ, the method would have to distinguish between the carbon in the fiber and that in the matrix material. However, AES is a useful tool for determining the elemental analysis of the fiber surface, but is not as powerful nor as common as X-ray photoelectron spectroscopy.

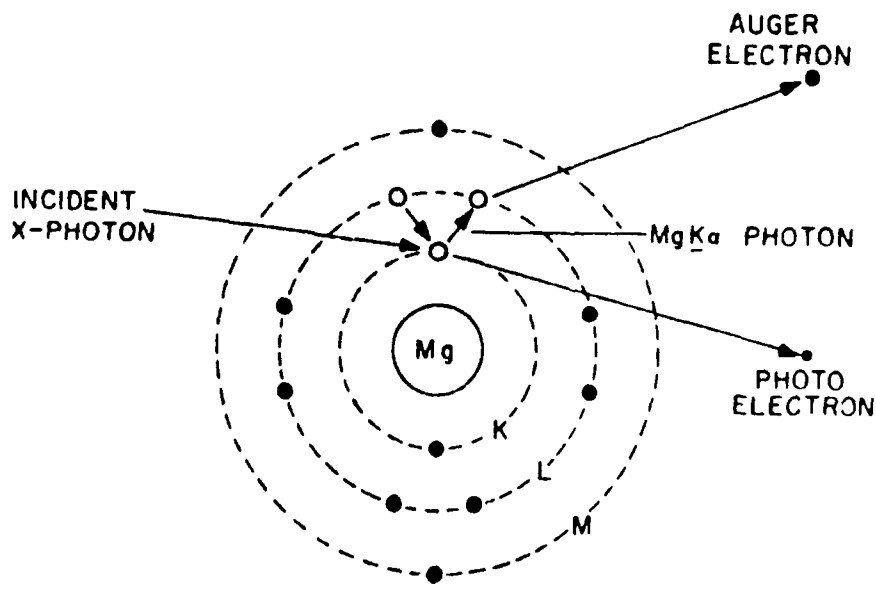


Figure 4. The bombardment of an atom with X-rays

#### 3.1.2.6 X-ray Photoelectron Spectroscopy (XPS or ESCA)

XPS is generated by the emitted photoelectrons when a sample is bombarded with monochromatic X-rays. As with Auger spectroscopy, the energy of the emitted electrons is



characteristic of the emitter and only the surface electrons can escape the sample surface. The bands created are both sharper and more intense than those for Auger spectroscopy. Resolution of XPS is as low as 120 nm—very small compared to the size of the fiber diameter at 7,000 nm. There is a virtual lack of problems caused by electrostatic charging. XPS has been used extensively to study carbon fibers both before and after surface treatment or sizing to determine the elemental analysis of the surface (21).

Unlike the carbon Auger spectra, the carbon photoelectron peaks contain a wealth of information such as the the substituent groups on carbon fibers. The  $C_{1s}$  peak is asymmetric at about 285 eV. As graphitization temperature increases, the band becomes narrower, indicating greater orientation within the fiber and less defects. Figure 5 shows XPS, Raman, and X-ray diffraction spectra for carbon fibers as the carbonization temperature increases (18).

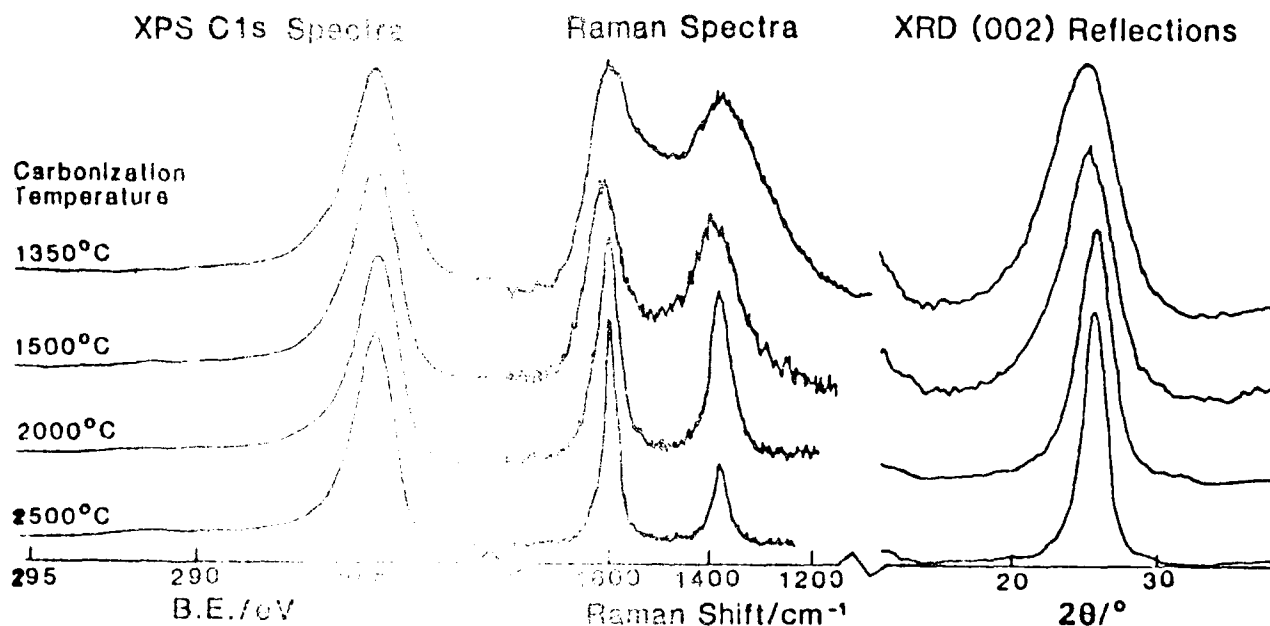


Figure 5. Spectra of carbon fibers at various carbonization temperatures

Bascom, in his work for NASA, has done extensive XPS analysis of PAN-based carbon fibers. The results show that these fibers contained carbon, oxygen, and nitrogen on the surface and that the amount varied between fiber types. The fibers studied included AS4 and XAS, both treated with the manufacturer's standard surface treatment. They are made from different PAN precursors. AS4 was composed of 84.3% C, 7.6% O, and 4.3% N, and XAS of 84% C, 7.6% O, 8.4% N (to a depth of 10 nm). Upon closer inspection, the following data was obtained:

Table 1. XPS analysis of graphite fiber surface chemistry

<u>Group</u>	<u>AS4</u>	<u>XAS</u>
COOH	none	trace
C=O	2.4	4.3
COX	2.8	3.6
COC		
COR		
COH	0.6	--
Heterocyclic N	1.6	3.6 (4)

XAS fiber clearly has greater functionality.

The Chinese have done an excellent study of the effects of various surface treatments a carbon fiber made in China using XPS. The treatments studied were: (#1) oxygen plasma; (#2) nitrogen plasma; (#3) anionic oxidation in 5% by weight NaOH; and (#4) a reflux treatment with 56% nitric acid. The change in surface chemistry for the various treatments was

Table 2. XPS analysis of fiber surface after treatment

<u>Group</u>	<u>COO</u>	<u>COOH</u>	<u>CO</u>	<u>COH</u>	<u>CH</u>
<u>BE* (eV)</u>	292.0	289.6	287.3	285.5	284.0
<i>Treatment on fiber:</i>					
<u>none</u>	none	3.4	6.4	16.5	73.7
<u>#1</u>	8.5	11.9	17.2	22.1	40.2
<u>#2**</u>	8	14	21	28	30
<u>#3**</u>	none	13	17	23	48
<u>#4**</u>	none	11	19	36	41

\*BE-Binding Energy

\*\*Data interpolated from graph.

The oxygen plasma surface treatment increased the amount of oxygen on the surface to two times that without treatment, and that of nitrogen to 1.5 times.

These researchers observed that the carbon on the surface of the fiber is in different chemical environments, and that different surface treatments give different surface groups. They could tailor

the fiber surface chemistry for compatibility with a given resin system. They have also shown that the functionality introduced on the fiber by surface treatment reaches a maximum and then no more groups can be added beyond that level (22).

Others have used unique signature elements such as  $\text{Ba}^{++}$  to tag the reactive oxygen on the surface to increase identification. It has been shown that on Type II fibers (high strength) that the number of sites on a  $(10\text{nm})^2$  area of the fiber was 1,900, while that on Type I (high modulus) fibers is only 550 (21). This confirms that high modulus fibers are more perfect and highly oriented because they have fewer defect sites with active oxygen.

From their XPS work, Denison and Jones have proposed a model of the fiber surface in which reactive sites occur at micropores. Their studies focused on the number of carboxylic acid groups per  $(10\text{ nm})^2$ , and found that with no surface treatment, there were about 300, but with 50% of the normal treatment used by Hercules, there were about 500. No further increase of carboxylic acid groups with treatment was found. The proposed micropore model is shown in Figure 6 (6).

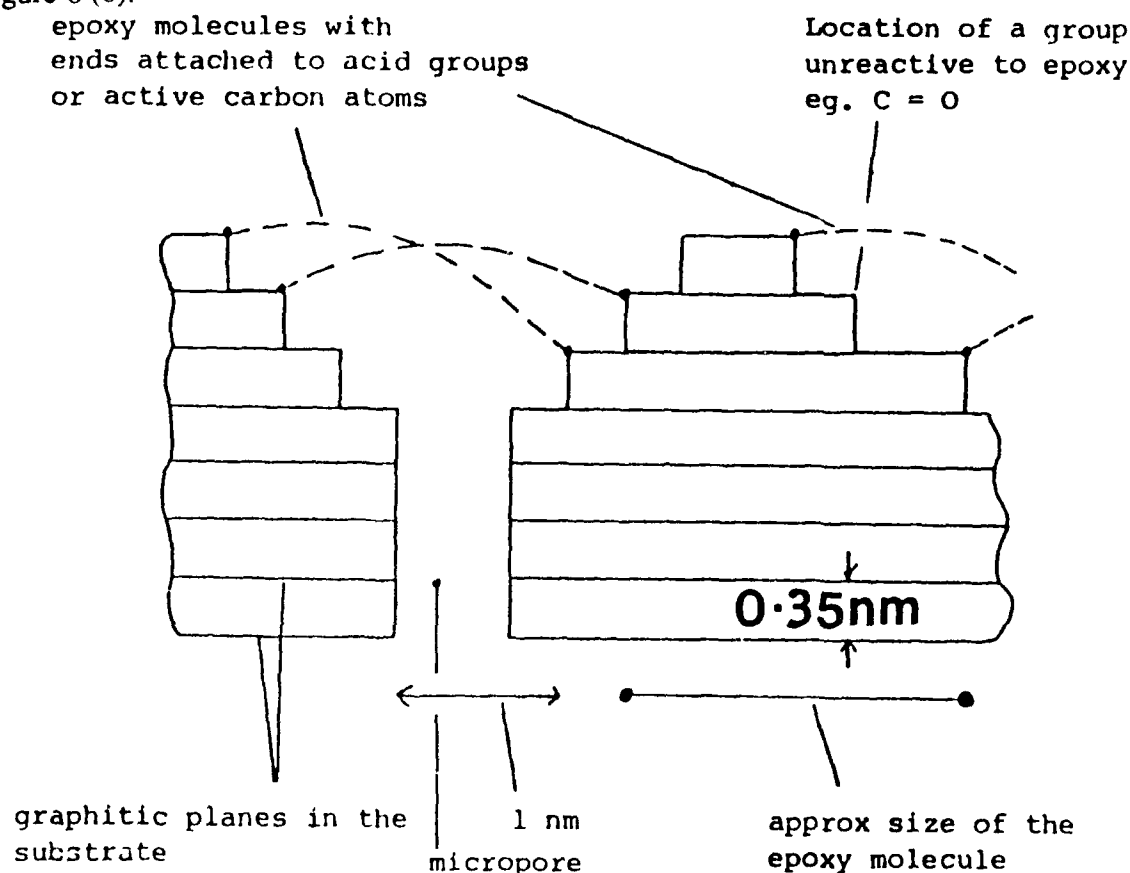


Figure 6. Schematic structure of the model interface

Carbon fibers have a complex morphology and surface chemistry which bear on the problem of adhesion to polymers. There are several ways to change the surface chemistry, and good

scientific methods to quantitatively measure those differences. While our understanding of carbon fibers is not complete, the means to further understand their nature is quickly becoming mature.

## 3.2 Matrix Polymers

### 3.2.1 Thermoset Polymers

For the past 20 years or more, thermoset polymers have been used as organic matrix materials. Thermosets are cured during processing into glassy, amorphous, three-dimensional networks of crosslinked polymeric chains. Thermosets include several polymers, the most common of which is epoxy. The uncured epoxy resin has very polar functional groups: the epoxy ring and amines. These polar groups make chemistry relatively easy with thermosets.

Reactions with carbon fibers and epoxies are hypothesized. Denison believes that carbon fiber surface carboxylic acid groups react with the unreacted epoxy rings at the surface to create ester linkages (6). Cooke claims that surface hydroxyl groups react with the epoxy ring to form ether linkages. Hydrogen bonding is also possible (7). (See Figure 7).

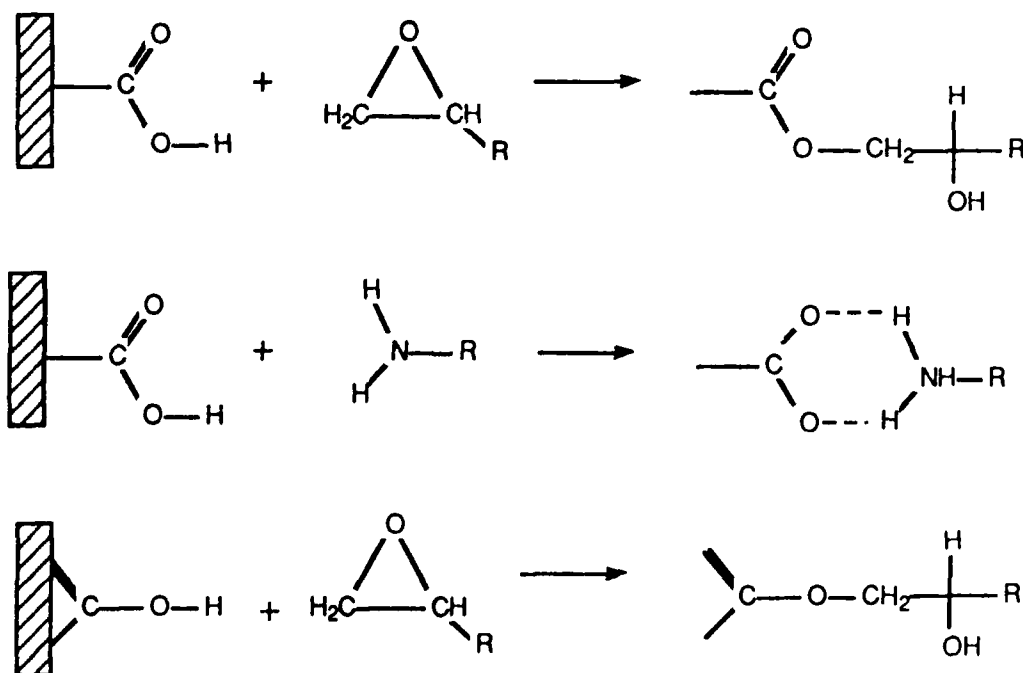


Figure 7. Reactions between epoxy resins and hardeners and carbon fiber surface groups

### 3.2.2 Thermoplastic Polymers

Of intense interest to the aerospace industry now are thermoplastic polymers. Thermoplastics are quite inert. Few chemically or electrically active groups are part of the polymer

chain and so they have low glass transition temperatures. Thermoplastic carbon fibers are generally made from poly(ether-ether-ketone), called PEEK.

Engineering thermoplastics such as sulfones, imides, and amides are surrounded by large carbonyl groups, which are electron donor or receptor groups. These polymer chains are highly crystalline with small micropores. The micropores are considered crucial, yet difficult to control in fiber micropores. See Figure 7.

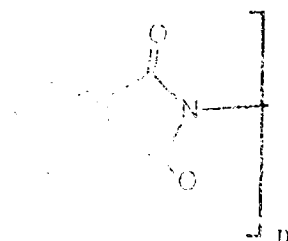
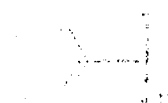
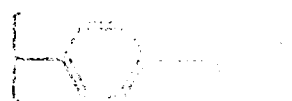


Figure 7. Sulfones

Later versions of carbon fibers, indicating higher modulus fibers, indicating that the

researchers had found a better Kevlar product. The new polymer is poly(aryl-ether-ether-ketone), called PEEK.

These polymers are composed of aromatic rings, which are electron donor or receptor groups such as C=O are often found in these polymers. Many thermoplastics have a high degree of crystallinity and a wide range of reactions. Long polymer chains are often terminated with sites in very small micropores, which many researchers consider crucial, yet difficult to control in carbon fiber micropores. See Figure 8.

Later versions of carbon fibers, indicating higher modulus fibers, indicating that the researchers had found a better Kevlar product. The new polymer is poly(aryl-ether-ether-ketone), called PEEK.

itself to increase adhesion. An example of chemical modification could be the addition of pendant groups, such as substituted methyls, which introduce a site for chemistry to take place. In general, however, the reaction kinetics are not as favorable between carbon fiber surfaces and thermoplastics as with epoxy systems.

Some thermoplastic polymers (e.g. PEEK) are semicrystalline, containing from 10 to 88% crystals. Crystallinity can effect mechanical as well as physical properties (such as resistance to solution or swelling in solvents). It has been discovered that PEEK crystals are stacks of lamellae 3-5 nm thick and grow laterally outwards in the radial direction from the nucleation point, which is often the fiber itself. This phenomenon is called *transcrystallinity* and has been documented by several researchers (23). The nucleation of spherulitic crystallites from the carbon fiber in fact dominates the morphology of APC-2. We think that the transverse crystals may act like little bolts securing the fiber in the matrix, and thus increasing the interfacial shear strength. Understanding crystallinity near the fibers can be very important in predicting mechanical properties of the composite as whole. (See Figure 9).

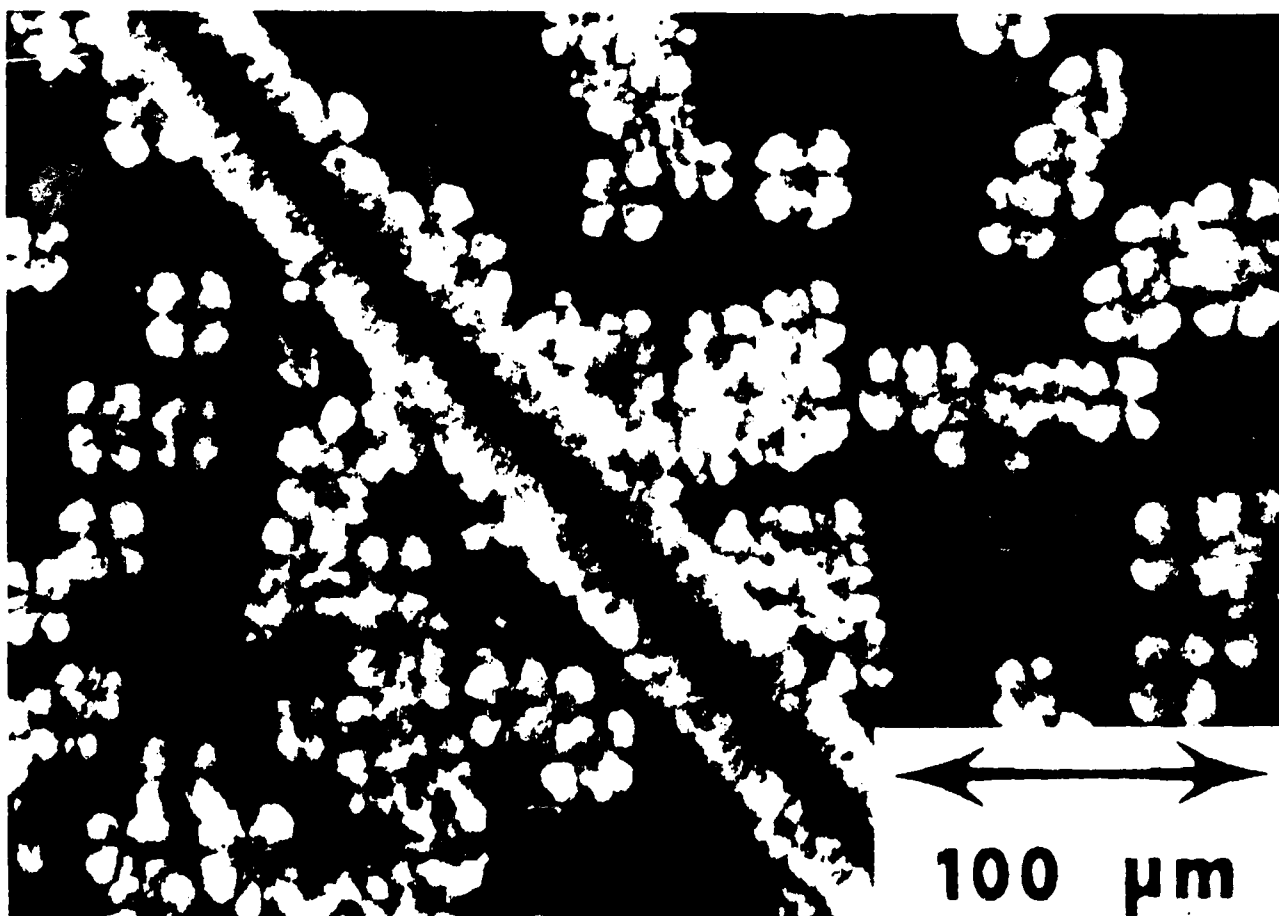


Figure 9. Photograph of transcrystallinity in PEEK  
Courtesy Dr. David P. Anderson, University of Dayton Research Institute

To date, most nonproprietary research in aerospace quality thermoplastic composite adhesion has been done on the extrusion grades of APC-2, presumably 150 grade. This is interesting because APC-2 has had no problems with poor adhesion. Other thermoplastic systems have much worse adhesion. HTA and PAS-2, both amorphous systems, have poorer adhesion.

The chemistry and morphology of matrix materials is also important in determining adhesion, but polymers are not as easy to study nor as well understood as graphite fibers.

## 4. Interface

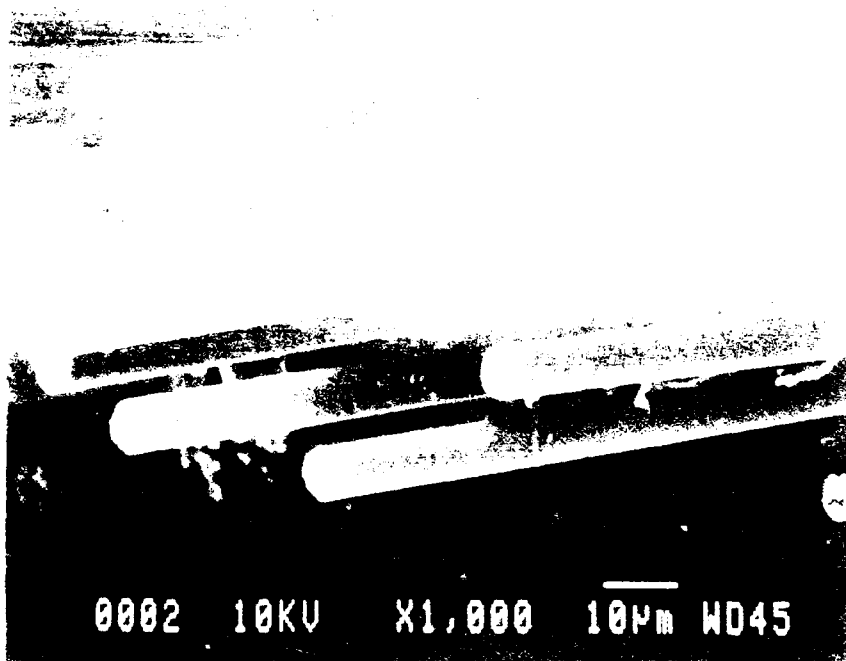
The interface is the exact surface where the fiber meets the matrix. On a molecular scale, this can be a very difficult area to define, particularly with chemical bonding, interdiffusion, and surface roughness complicating the issue. Often, the interface is thought of as a separate third phase, consisting of the actual interface, outer layer of the fiber, and the matrix near the interface. This area is called the *interphase*. The interphase, therefore, may extend only for a few microns from the fiber at the most. The weakest part of the interphase determines the level of stress transfer and the distribution of the stress concentrations at the fiber ends during failure and debonding (4).

### 4.1 Observation of the Interface

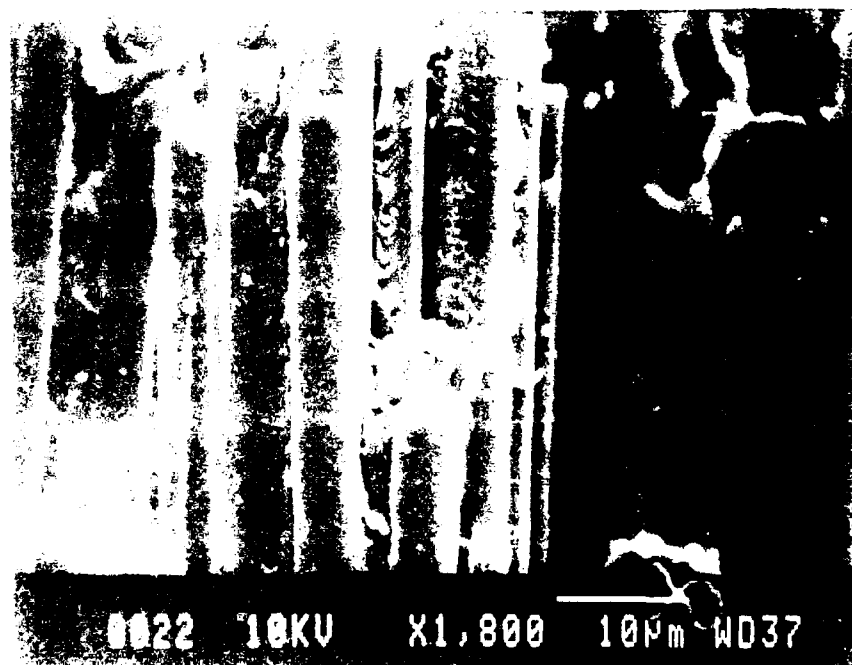
#### 4.1.1 Scanning Electron Microscopy

One of the most fundamental ways of assessing the interface is to look at a failed specimen in the SEM and observe the degree of adhesion between the matrix and the fibers. Figure 10 shows SEM pictures of thermoplastics and epoxy resins with different graphite fibers. It is easy to see that some of the fibers appear smooth and some appear "fuzzy" or "messy" where the matrix material has clung to the fiber. If the interfacial strength is great enough, the composite will fail in the bulk matrix material rather than at the interface. In that case, matrix polymer will stick to the fiber making it appear messy in the SEM. If not, the bare fiber will appear smooth. However, very thin layers of polymer may remain on the fiber and it will still appear smooth. The fibers may also appear smooth if a size has been deposited. SEM alone cannot detect this. Although SEM imaging is not the unequivocal method of determining interfacial adhesion, it is very common, easy to perform, and a good indication of adhesion along with mechanical testing and theoretical calculations.(24).





a.



b.

Figure 10. SEM photomicrographs of composite fracture surfaces  
 a. KIII/AS4 (amorphous thermoplastic/PAN-based graphite 16 July 87)  
 b. HTA/IM8 (amorphous thermoplastic/intermediate modulus PAN-based graphite)



Figure 10, continued

- c. 8551-7/IM7 (rubber toughened epoxy/intermediate modulus PAN-based graphite)
- d. PAS-2/AS4 (amorphous thermoplastic/PAN-based graphite)
- e. HTX/IM8 (semicrystalline thermoplastic/intermediate modulus PAN-based graphite)

SEM has also been used to investigate transcrystallinity in thermoplastic composites. An etch of a potassium permanganate solution on APC-2 preferentially washes out the amorphous regions leaving the crystalline areas above the surface of the sample. Then, the SEM is used to observe the crystalline patterns (see Figure 11). At slow cooling rates of the composite from the melt temperature of the polymer, very little nucleation occurs, so the crystallites are larger. At higher cooling rates, the crystals are smaller and more numerous.

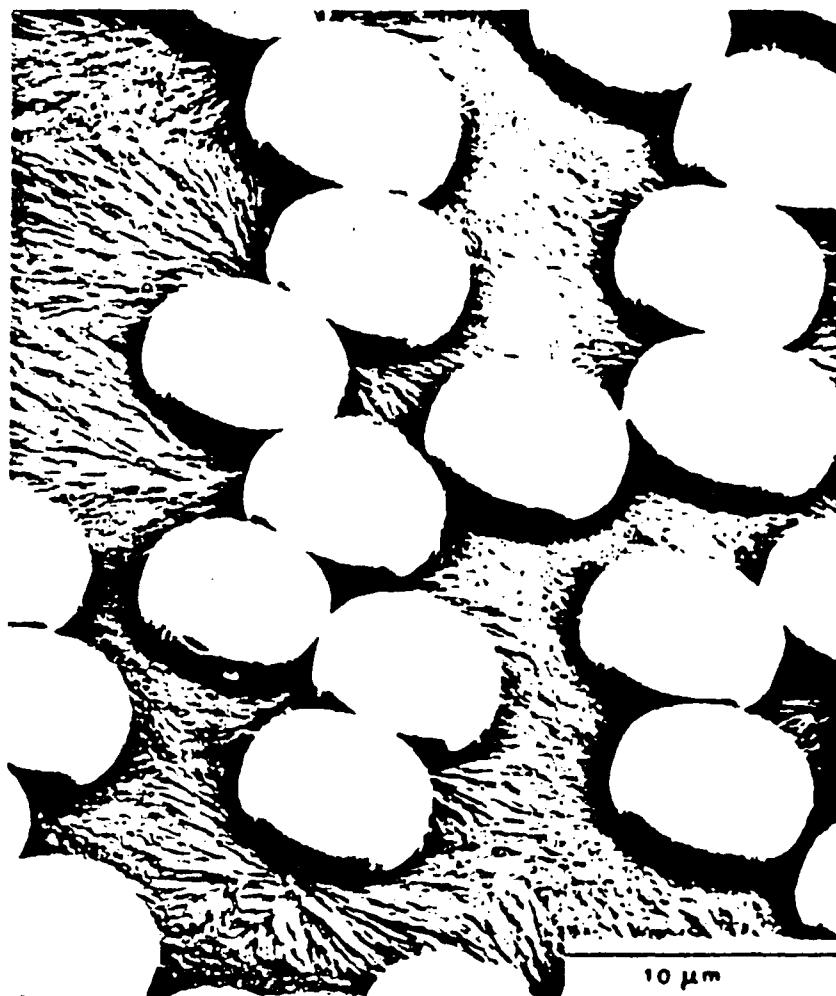


Figure 11. SEM photomicrograph of etched cross section of APC-2 laminate cooled at 15°C/min

Peacock has discovered that different types of fibers inspire different nucleation of transcrystallinity. In general, Type I fibers are better nucleants than Type II. This implies that the crystals must nucleate from the graphitic basal plane surface, rather than from the edges or other imperfections (25). In addition, high strength fibers experience nucleation most often where two fibers are close together. Why would this occur? Resins shrink during cure and cooldown putting

normal residual compressive stresses on the fiber. These stresses are greatest on the fiber where they are closest together. So transcrystallinity in Type II fibers must be effected by residual thermal stresses at the interface (26).

These results have been matched with mechanical properties. Transverse flexural tests and SEM of three systems (APC-2/AS4, PEEK/Type II fiber, and PEEK/Type I fiber) were executed. Of course, ICI has optimized the interface in APC-2, but the results are still useful:

Table 3. Transcrystallinity and mechanical properties

<u>System</u>	<u>90° Flex Strength (KSI)</u>	<u>SEM Fiber Appearance</u>
APC-2/AS4	22.1	messy
PEEK/Type II	7.78	smooth
PEEK/Type I	11.1	both smooth and messy

Knowing that the Type I fibers have greater transcrystallinity nucleation than Type II, the author determined that transcrystallinity may indeed improve adhesion, but is not, in and of itself, a sufficient mechanism for achieving excellent fiber/matrix adhesion in non-optimized systems (23).

#### *4.1.2 Energy-Dispersive Spectroscopy (EDX)*

Scanning electron microscopy imaging is a good way to look at the interface, but it does not quantify its characteristics. EDX might help identify the elements present at the interface, but on closer inspection, this method has many problems. Although resolution is as small as 6 nm (less resolution than SEM), most EDX machines use windows which prevent identification of elements of lower atomic number than sodium. Since organic matrix composites are primarily carbon, hydrogen, oxygen, and nitrogen, composite chemistry cannot be detected. Even a windowless machine would pick up almost exclusively carbon, which would not differentiate between the fiber and the matrix. In any case, hydrogen could not be detected. When using a machine with low voltage, the depth from which the X-rays would emanate would be from a considerable distance beneath the specimen surface. It is easy to determine that examining either fiber surfaces or fracture surfaces using EDX would be fruitless (27).

#### *4.1.3 Secondary Ion Mass Spectroscopy*

SIMS can detect very thin layers of polymer left on the fiber surface after a failure. Some British academicians exposed Courtaulds XA fiber to three different oxidative surface treatments and then used SIMS to analyze the fracture surfaces of composites made from both treated and untreated fibers. SIMS detected thin layers of polymer remaining on the surface treated fibers, but not on the untreated one. This corresponds to increases in interlaminar shear strength. In addition, the ion maps generated helped to reveal the true failure mechanism (16).

## 4.2 Interface Impact on Composite Properties

Throughout this discussion it has been asserted that the interface can effect the properties of the composite material, but how and why? Most importantly, the interface between the fiber and the matrix is absolutely critical for the transfer of stress from the matrix to the fiber. When a load is applied to the composite, it is essentially applied to the matrix. Since the matrix is not as strong or stiff as the fibers, without transfer of the load to the fibers, the composite will fail much below what would be expected for the composite--at the failure strength of the polymer. With a "good" interface, the load can be transferred to the stronger fibers greatly increasing the strength of the composite. Good is a relative term because it is sometimes desirable to have a less than perfect interface.

Exactly how the interface plays its role in mechanical properties is quite complex. In  $0^\circ$  tension failure, when the first fiber breaks, the load is transferred through the interface to the neighboring fibers. A large shear stress concentration builds up at the fiber end which may induce failure of the other fibers. It may also cause shear debonding of the broken fiber at the interface. If the interface is too strong, failure of the fiber will result in catastrophic failure of the brittle composite. Failure of the interface by shear will allow dissipation of stress and energy and add additional strength to the composite. Therefore, the interface must be strong enough to allow stress transfer, but weak enough to fail in shear. In addition, energy from an impact can be dissipated by debonding the fiber in shear rather than actually damaging the composite. Hence, an increase in fracture toughness occurs.

In  $90^\circ$  tension or flex, the fiber/matrix interface is in tension. Therefore, the composite will fail at the weakest area--the fiber, the matrix or the interface. Interfacial tension failure is the most probable source of transverse crack initiation, and therefore dominates  $90^\circ$  tensile strength. If the specimen does fail at the interface, as can be ascertained by SIMS or SEM, the interfacial tensile strength is the  $90^\circ$  tensile strength. It is important to note that interfacial tensile strength is not the same as interfacial shear strength, which is the most often studied mechanical property of the interface.

The interface can have a huge impact on the shear strength of a composite if the failure mode is interfacial debonding. If so, the material shear strength is the interfacial shear strength. However, failure can occur in either the matrix or the fiber. If shear failure is in the matrix, the shear strength of the composite is that of the matrix. If failure is in the fiber, then only increasing the shear strength of the fiber will help. In graphite, fiber failure is not common because of the great degree of imperfection in the orientation of the crystallites. However, in high modulus fibers, this mechanism becomes more likely.

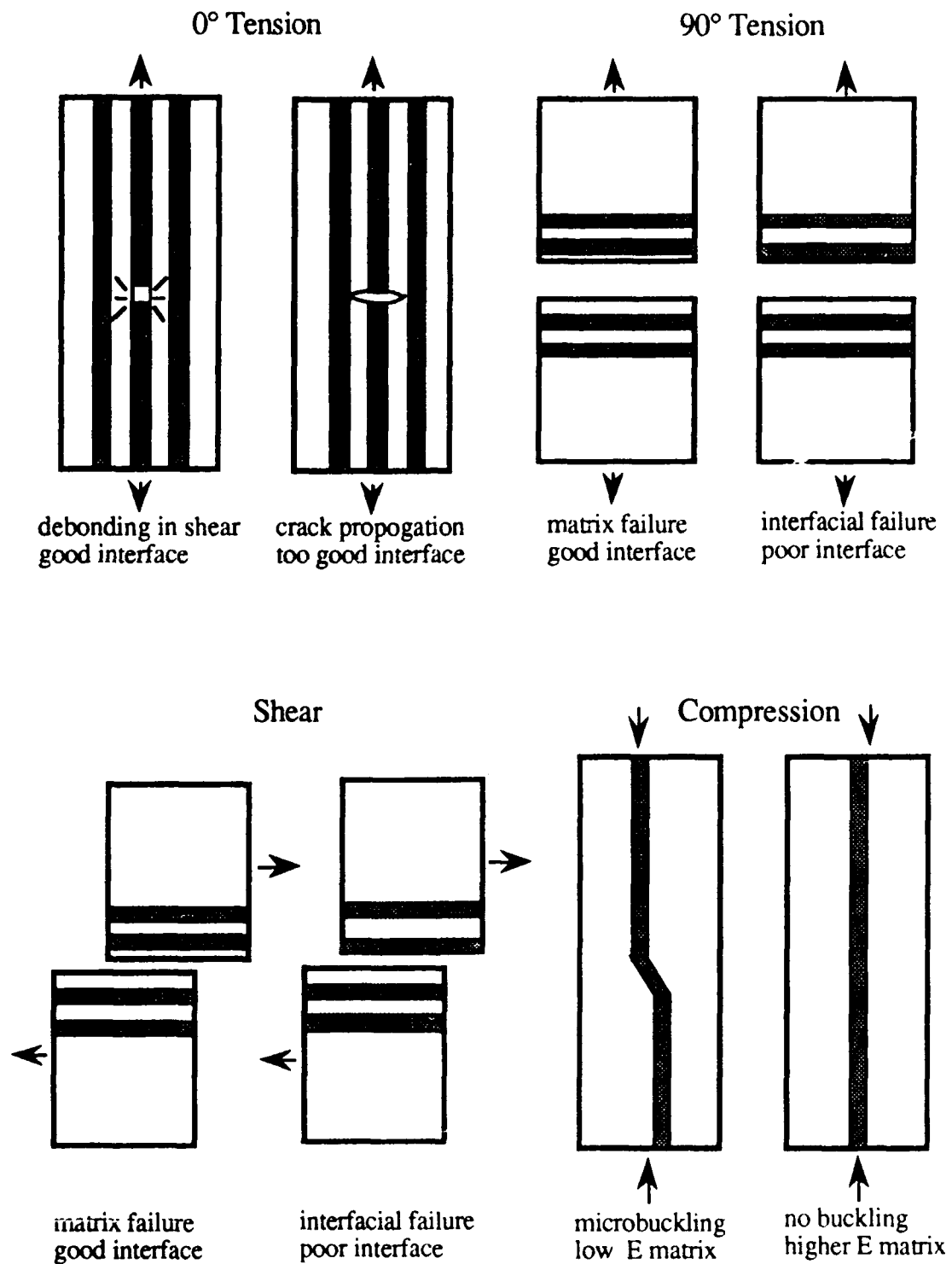


Figure 12. Interface impact on composite properties

Currently, it is believed that 0° compression strength is determined by laminate buckling stability, but it is still not well understood. It has been discovered that higher modulus matrices give greater compression strengths, probably because the matrix keeps the fiber from buckling. Although little work has been done in the area, Bascom and Drzal suggest that a stiff interphase region may improve composite compression strength. However, this would probably decrease toughness (1).

Dr. Drzal has done a study of how sizings effect mechanical properties which illustrates some of the concepts stated above. In his study, composites were made with a diglycidyl ether of Bisphenol-A and m-PDA. One Hercules fiber was used, AU4. When treated with Hercules standard surface treatment, the fiber is called AS4, and when also sized with a 200 nm thick epoxy compatible size it is called AS-4C. The results of the mechanical test are as follows:

Table 4. Variation in mechanical properties with fiber surface treatment and sizing

<u>Fiber</u>	<u>IFSS (KSI)*</u>	<u>Failure mode*</u>	<u>SBS (KSI)</u>	<u>0° T (KSI)</u>	<u>0° C (KSI)</u>
AU4	5.4	interface	3.8	170	87.6
AS4	8.9	interface	9.0	212	84.3
AS-4C	11.8	matrix	8.8	136	99.5

\*As determined from the embedded interfacial shear test.

Based on the rule of mixtures which assumes a perfect interface, all the values of 0° tension and compression should be the same, yet they are not. The only possible explanation is that the adhesion at the interface changes with surface treatment and sizing in this material system. The transfer of stress from fiber to fiber seems to become more efficient when the fiber is surface treated, so the tensile strength increases. AS-4C has a different failure mechanism, though. The very high IFSS causes the fiber not to debond as the others do. Instead, the broken fiber starts a matrix crack which propagates through the composite, giving lower tensile strength.

In 0° compression, Drzal believes that the sizing provides a stiff sheath which keeps the fiber from buckling, and thus increases compression strength. Apparently, interfacial adhesion has little effect on compression strength. In short beam shear strength, the samples of AU4 and AS4 did fail in shear, but the AS-4C failure is more complex. The size apparently changes the failure mechanism. The surface treatment increases the shear strength, which is illustrated by the IFSS increase (28).

This study also clearly points out that the rule of mixtures for predicting macroscopic composite properties is not sufficient. One new model has been introduced which accounts for a third interphase region simply by adding another term to the rule of mixtures equations. The properties of the interphase are deduced from differences in the original rule of mixtures calculations and the actual properties as ascertained by dynamic mechanical means (29). Other models are available, but are not in common use. Empirical analyses are a start, but are not enough. An actual scientific understanding of the fiber surface and matrix material could lead to a more universal model which will provide insight into techniques to improve the interface.

Changes to the interface, such as the introduction of water in epoxy materials, could also change properties. In that case, the matrix near the fiber is plasticized, likely increasing toughness and decreasing compression strength. In addition, properties such as electrical and thermal conductivity are probably changed with changes in the interphase region (30), but little work has been done in that area. Succinctly, while trying to improve one facet of the composite properties by improving adhesion, other properties may have to be traded . It is a careful balance for a materials engineer to maintain.



## 5. Interfacial Shear Strength Tests

### 5.1 Single Fiber Pull-out Tests

Single fiber pull-out tests have been used to test the fiber matrix interface. Both the IFSS and the subsequent frictional stress associated with the sliding of the fiber along the debonded area can be determined. The test is performed by embedding a fiber of length  $L$  in a cylinder of matrix material. Then the fiber is pulled out of the matrix. The initial force to detach the fiber and that required to slide the fiber are recorded. This process is repeated at increasing  $L$  until the fiber fractures when it is pulled. A graph of  $L$  versus the debonding force  $F_d$  yields a straight line which has a slope equal to the shear debonding strength (the IFSS). The geometry of the matrix can also be a disk rather than a cylinder. In either case, the meniscus of the polymer can cause stress concentrations that increase the data scatter. One way to eliminate the stress concentrations is to cure a drop of resin onto the fiber and pull the fiber out of the drop. This method has been shown to reduce data scatter. Figure 13 shows a schematic of two geometries of the pull-out test (1).

Piggott and his colleagues have defined three ways in which interfacial debonding occurs in the single fiber pull-out test. First, it can occur across the whole embedded length of the fiber at the same time. This is the condition assumed in the single fiber pull-out test. Second, the failure can be progressive starting at the surface of the disk where the IFSS is maximum and progressing to the far end of the fiber. In this case, the plot of  $L$  versus the  $F_d$  yields a logarithmic-shaped curve, which is a function of  $E_m$ ,  $E_f$ ,  $V_m$ , the diameter of the fiber, and the diameter of the polymer block. The third possibility is that the brittle failure of the interface is governed by the energy criterion (an energy balance). Therefore, the shape of the curve might yield an understanding about how the interfacial failure in a particular system happens.

Measurement of the frictional forces after debonding is important in assessing residual thermal stresses. Piggott and Dai have shown that residual stress has no effect on an epoxy/glass debonding stress, but does increase the frictional stress (31). Friction shear stress at the interface,  $\tau_f$ , is governed by a simple equation:

$$\tau_f = \mu P$$

where:

$\mu$  = coefficient of friction

$P$  = the normal pressure on the system.

#### Pull-out method

$$\tau = \frac{F}{A} = \frac{F}{\pi d l}$$

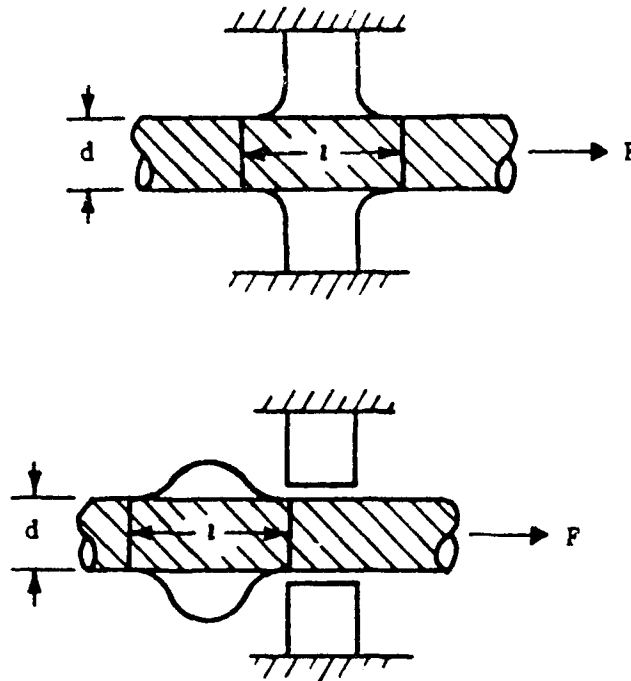


Figure 13. Schematic of single fiber pull-out method

The frictional IFSS increases with increasing pull-out distance because the strength of the fiber decreases (since it is governed by defects). The slope of the curve of  $L$  versus  $F$  at the point where the fiber emerges from the polymer is called the pressure due to matrix thermal and cure shrinkage,  $P_0$ . Thus, the author suggests a way to measure residual thermal stresses empirically (32).

There are several problems with the single fiber pull-out test. For one, the fiber embedded length must initially be small enough so that the fiber doesn't fracture before debonding. In addition, the fibers are small, difficult to clasp during the test, and the force is tricky to measure. The fiber must be perfectly aligned and very clean to get good results. Finally, this is not a true composite test, since only one fiber is used. The stress transfer from one broken fiber to another is not taken into account. Single fiber pull-out test may be useful in measuring interfacial residual stresses, but it is most useful for comparative purposes to determine if the surface treatment or sizing has indeed improved the interfacial shear strength.

## 5.2 Embedded Interfacial Shear Method

### 5.2.1 Method

The embedded interfacial shear test, which was originally proposed by Kelly, has become a standard method for quantitatively measuring the interfacial shear strength. In particular,

Larry Drzal of Michigan State University and Willard Bascom formerly of Hercules Aerospace have done extensive research using this method.

In Dr. Drzal's adaptation of the test, a single very clean fiber is embedded in a brittle, transparent, birefringent matrix material in a miniature dogbone. The specimen is shown in Figures 14 and 15. The matrix material must be of lower modulus than the fiber. In all his early work, Drzal used EPON 828 with an m-PDA curing agent as the matrix material. Next, the sample is put in tensile stress. When viewed under crossed polarizers, as the stress increases, a bright fringe appears around the fiber. Then the fiber begins to break, and a node in the bright fringe appears at the fiber end. As the stress increases, the fiber continues to break into shorter and shorter lengths. The nodes move away from the ends, but leave a uniform sheath of birefringence. If the bond is good, this sheath will persist indefinitely after the stress is relieved. Figure 16 shows a typical birefringence pattern in a well-bonded specimen (1).

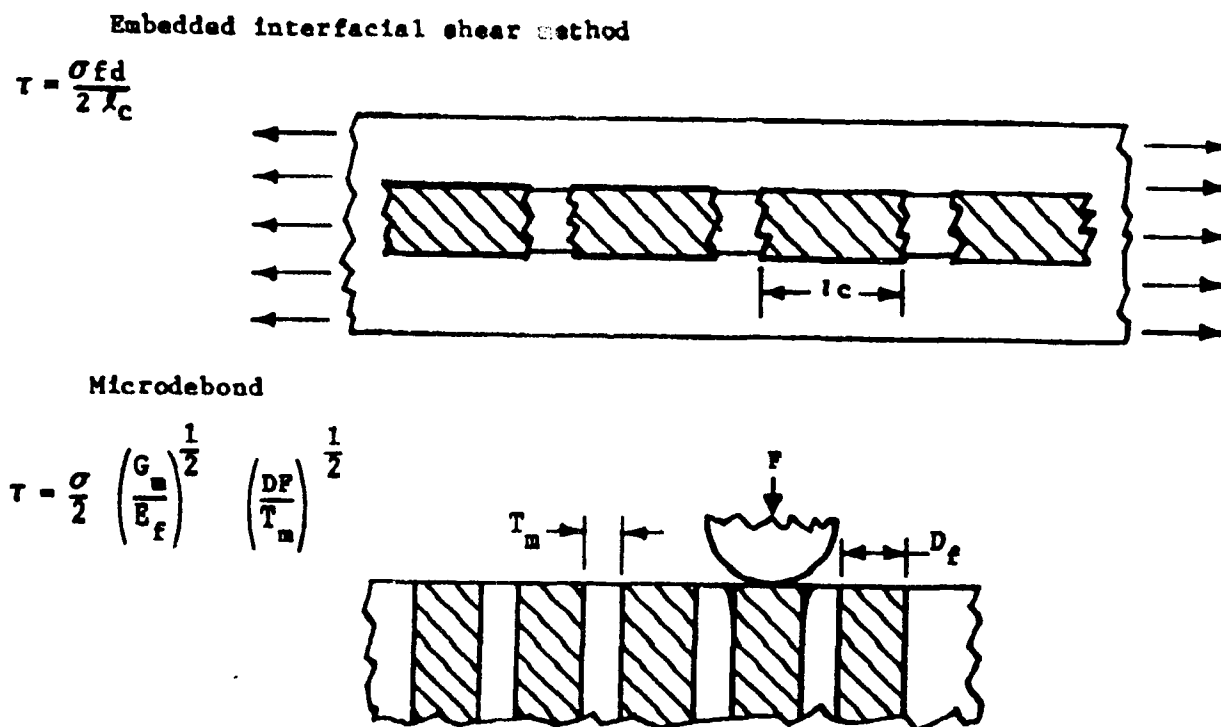


Figure 14. Schematics of embedded interfacial shear and microdebond methods

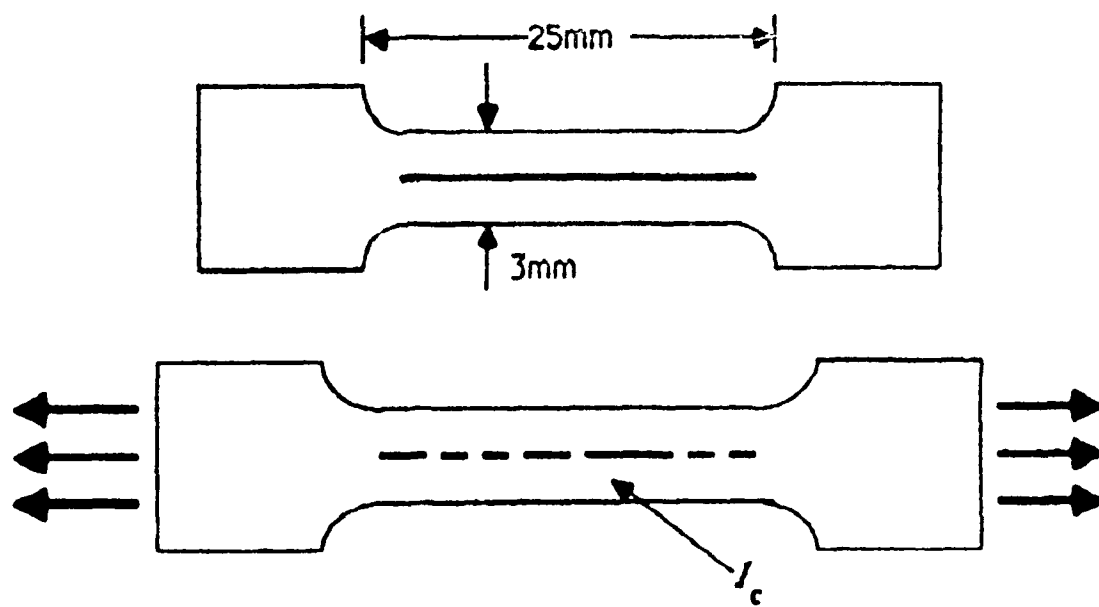


Figure 15. Geometry of embedded interfacial shear test specimen

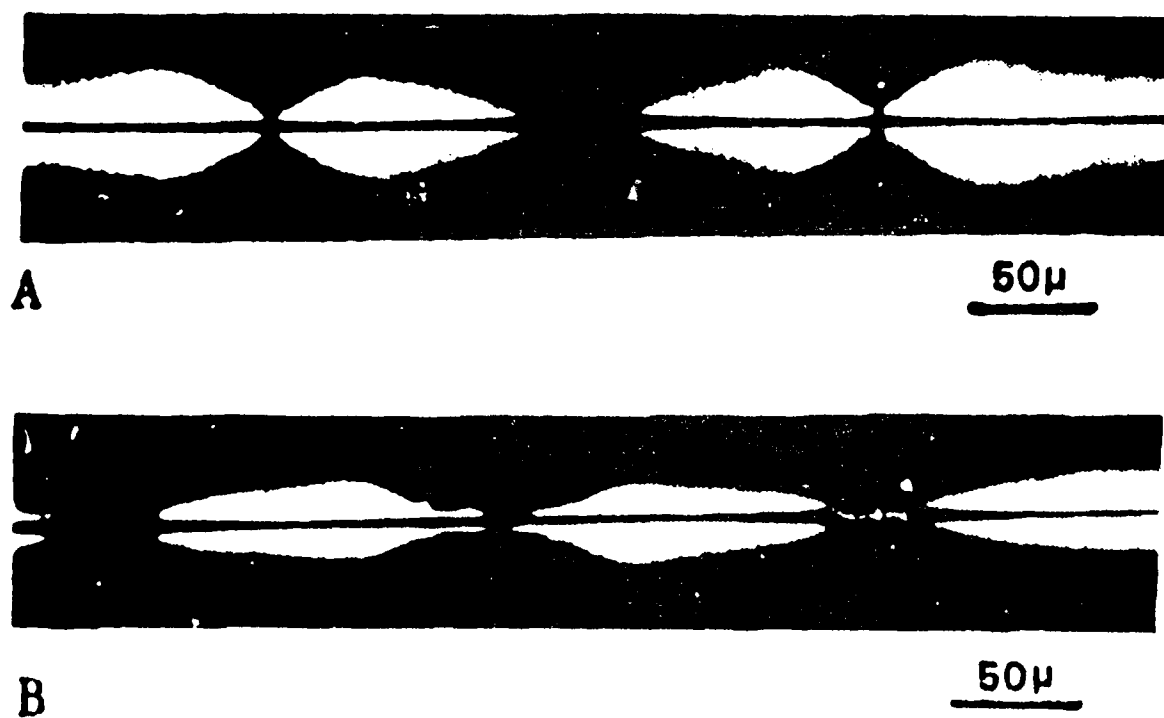


Figure 16. Birefringence in well-bonded XAS fiber in polycarbonate

In a poorly bonded composite, the sheath develops but it is relatively low in intensity. It disappears after the tension is relieved. This is an indication of the "unzipping" of the interfacial bond. Hence, viewing of the sample under crossed polarizers offers a qualitative way to assess the interfacial strength (4).

But quantitative data may be obtained, too. According to Cox's shear lag model for a well-bonded system, the shear stress is greatest at the fiber ends and reaches zero at some distance from the end. The tensile stress is zero at the fiber ends, and then reaches its maximum at that same distance. That distance is  $l_c/2$ , where  $l_c$  is the critical length for stress transfer. The relationship between the IFSS,  $\tau_c$ , and the critical length is:

$$\tau_c = (\sigma_c/2) (d/l_c)$$

where:

$\sigma_c$  = fiber tensile strength

$d$  = the fiber diameter (33).

However, the strength of a fiber is actually a distribution of strengths and can be reduced to a mean and variance using Weibull statistics. Then the expression for the mean  $l_c$  is substituted for the simple  $l_c$  to give the result:

$$\tau_c = (\sigma_c/2\beta) \Gamma(1-l_c/\alpha)$$

where:

$\alpha$  is the shape factor for the Weibull distribution

$\beta$  is the scale factor for the Weibull distribution

$\Gamma$  is the Gamma function (11).

If the log of  $l_c$  is plotted versus the probability of fiber failure, a linear plot should result. Bascom and Jensen have found that when making such plots for PAN-based Hercules fibers in EPON 828/m-PDA, the graph has not one but two linear regions, each with distinct shape and scale factors. This phenomenon indicates that rather than one type of flaw which controls the fracture of fibers, there are two (34). In practice, a normal distribution for the fiber strengths has been used with good results, although it is not statistically accurate. In that case, the data can be reduced by the equation:

$$\tau_c = \sigma_c d / (2 l_c)$$

Notice that as  $l_c$  or  $l_c/d$  (called the critical ratio) decreases,  $\tau_c$  increases.

Using a different analysis model, Whitney and Drzal have calculated that the maximum IFSS occurs at about  $0.2 l_c$ , not at the fiber ends as previously predicted. Figure 17 shows tensile and shear stresses at the fiber ends (35).

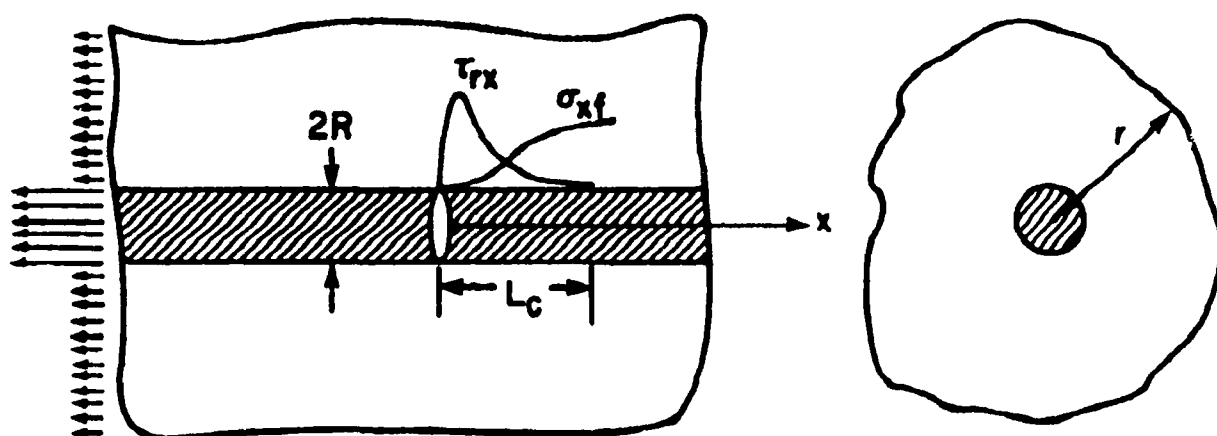


Figure 17. Schematic of tensile and shear stress concentrations at the fiber ends

### 5.2.2 Data

Drzal and his colleagues at Michigan State University have performed this test on PAN- and pitch-based fibers to compare differences. The matrix material used was similar to before-- Dow epoxy DER#331 and m-PDA hardener. The results IFSS tests were:

Table 5. IFSS of PAN and pitch-based fibers in DER#331

<u>Fiber</u>	<u>Surface treatment and size</u>	<u><math>\tau_c</math> (KSI)</u>
Apollo 38-750	no treatment or size	3.25
Apollo 38-750	no treatment epoxy sized	7.06
Apollo 38-750	treated and epoxy sized	8.68
P-25	no treatment or size	2.0
P-55	untreated, sized with UC-318	1.56
P-75S	treated and sized with UC-320	1.79
P-100	untreated, sized with PVA*	1.31

\*PVA-poly(vinyl alcohol)

The Apollo fibers are PAN-based Hysol-Grafil product, while the P denotes a pitch-based fiber by Amoco (formerly Union Carbide). The authors report that the size on the Apollo fibers changed the failure mode from crack propagation along the interface to a matrix failure. The first

thing to notice is that even with surface treatment and sizing, adhesion is much lower in pitch than PAN-based fibers. Next, as modulus increases, IFSS declines, but with surface treatment, it again increases. This is explained by two factors. First, as modulus increases, fewer defects occur at the fiber surface, and there are less active sites to be attacked by either the size or the resin. Second, surface treatment adds additional active sites to the fiber, reversing the effect of rising modulus (36).

Bascom conducted a very comprehensive study of IFSS of thermoplastic/graphite composites in 1986-87 for the Navy. The results are summarized below:

Table 6. IFSS of PAN-based fibers in thermoplastic matrices

<u>Fiber</u>	<u>Polymer</u>	<u><math>l_c</math> (mm)</u>	<u><math>\tau_c</math> (KSI)*</u>
AS4	PC	0.74	2.40
AS4	PPO	0.83	2.14
AS4	PEI	0.64	3.78
AS4	PS	0.83	2.14
AS1	PC	0.95	1.89
AS1	PEI	0.65	2.77
XAS	PC	0.36	4.61
XAS	PPO	0.37	4.49
XAS	PEI	0.36	4.61

\*Calculated by this author from data in the reference.

PPO - Poly(phenylene oxide)

PEI - Poly(etherimide)

PS - Polystyrene

PC - Polycarbonate

All of the fibers were unsized and had the manufacturers' standard surface treatment. From the data, it is clear that Hysol-Grafil's XAS fiber was much better in thermoplastic adhesion than the Hercules fibers. This was confirmed by the residual birefringent sheath present on the XAS samples, but not on the AS1 or AS4 samples. The XPS surface chemical analysis was presented in Table 1 and found to have a greater percentage surface functional groups.

Also in this study, the effects of several sizings with polycarbonate matrix material and AS4 fibers were investigated. The sizings included:

W-size (epoxy-based Hercules proprietary size);

epoxy anhydride;

polyimide;

aminopropylsilane;  
polycarbonate; and  
phenoxy (PKHT by Union Carbide).

Only the phenoxy sizing improved adhesion significantly, reducing  $l_c$  from 0.74 to 0.54, which corresponds approximately to a 0.9 KSI increase in IFSS.

Finally, the effects of surface treatment on the PC/AS4 and PC/XAS interface were studied. The surface treatment was the normal proprietary treatment used by Hercules. Levels of 0, 1, and 4 times the normal treatment were tried. The results were:

Table 7. IFSS variation with surface treatment

<u>Fiber</u>	<u>Treatment</u>	<u><math>l_c</math> (mm)</u>	<u><math>l_c</math> (KSI)*</u>
AU4	none	0.86	2.07
AS4	1 times	0.74	2.40
AS4	4 times	0.89	2.0
XAU	none	0.57	2.91
XAS	1 times	0.36	4.61

\*Calculated by this author from data in the reference.

Clearly the fiber manufacturers have optimized the level of surface treatment, and additional treatment adds nothing and perhaps even damages the fiber.

Bascom was unable to explain the reason for the difference in adhesion of XAS and AS4 to thermoplastics from his data. He states:

There does not seem to be any specific chemical reason for the differences. The XAS and AS4 exhibited distinctly different adhesion strengths to very chemically different polymers. Only in the case of the thermosetting polymers-the epoxies-was the adhesion strong for both XAS and AS4. This fact raises the issue of polymer conformation at the surface. . . The XPS analysis suggests that the XAS and AS4 surfaces are chemically different and this difference may be such that all of the thermoplastics adsorb on the XPS in configurations that favor strong bonding. . . Quite possibly, it is not the difference in chemical composition but in the spatial distribution of chemical groups that effect conformation.\*\*\*\*

\*\*\*\*The possible role of polymer surface configuration in the adhesion of the thermoplastics was suggested to the author (Bascom) by Prof. L. T. Drzal, Michigan State University and Dr. T. M. Johnson, Phillips Petroleum Co., Bartlesville, OK.



Bascom goes on to say that studies of polymer conformation on carbon fiber surfaces presents some formal difficulties (4).

### 5.2.3 *Comments on the Embedded Interfacial Shear Test*

We must consider several assumptions when conducting an embedded interfacial shear test. That the interfacial shear strength is constant over the entire length of the fiber is valid only when the matrix flows or yields at the interface. If the failure takes place in the matrix instead, the IFSS has not been tested. Instead the shear yield strength of the matrix material was tested. This will not occur if:

$$\sigma_f \geq 3\sigma_m \quad (34)$$

If failure in a system does occur in the matrix, modification to the fiber surface will not improve IFSS. When conducting this test, the researcher must be careful to note the failure mechanism.

It is possible that the fiber does not fragment completely before the matrix breaks. In that case, the critical aspect ratio calculated will be too large, and the IFSS will be underestimated (37). Finally, it is noted by Bascom and Jensen that  $\sigma_c$  varies with length. That means that as the test progresses and the fiber fails at its weakest point, the fiber tensile strength increases. To be absolutely accurate, the  $\sigma_c$  of the fiber at  $l_c$  must be measured independently (35). Also, this test method, like the single fiber pull-out test, is not a composite test.

The final problem is the matrix material must be transparent and birefringent to see birefringence. Engineering thermoplastics are not usually transparent. If the engineer needs only the critical length, acid digestion of the sample will extract the fiber fragments from an opaque matrix, but observation of the failure is not possible.

Although the embedded interfacial shear test is not a perfect test and is difficult to perform and to properly reduce the data, it is the state-of-the-art method of measurement of interfacial shear strength. Data from this test are not absolute, but are very good for comparative analysis.

## 5.3 Microdebond Test

A new way of measuring the interfacial shear strength has been developed in the past two years by Dr. John Mandell while at MIT. Microdebonding involves indenting the fibers of a polished composite cross section at increasing force until debonding is detected under a microscope. The interfacial shear strength is calculated from the debonding force using finite element analysis. This model takes into account the fiber diameter, spacing to the nearest neighboring fiber, residual thermal stresses, and the mechanical properties of the fiber, matrix and far-field composite. This is the only method of direct measurement of the IFSS which is performed on a composite material.

Under Lockheed's contract with the Air Force, "Manufacturing Science of Complex Shaped Thermoplastics," MIT has performed the microdebond test on several thermoplastic composite materials with these results:

Table 8. Microdebond testing of thermoplastic matrix composites

<u>Material</u>	<u><math>\tau_c</math>(PSI)</u>
3501-6/AS4	7,053
Radel C/T650-42	7,016
APC-2/AS4	6,987
Cypac 7005/G30-500 (fabric)	6,152
Torlon/T500	5,131
PAS-2/AS4	4,862
PEEK/AS4 Cowoven	4,478
PAS-2/IM6	3,053

Of the materials tested, only Radel C/T650-42 and APC-2/AS4 have comparable interfacial shear strength with the state-of-the-art epoxy (38). Lockheed does not attempt an explanation. These numbers cannot really be compared to those deduced from the embedded interfacial shear test. The tests are very different. Data from the microdebonding are only good for comparison to like data.

Although this is a new method, it appears to be valuable to the engineer for practical data. First, any matrix material can be used, not just transparent, birefringent materials within a certain range of strain-to-failure values. Second, painstaking sample preparation is not necessary, simple cutting and polishing is sufficient. And finally, the test is more likely to reflect realistic conditions since it is performed on a composite rather than a single fiber. Of course, the data are only as good as the data reduction scheme.

## 6. Summary and Conclusions

The interphase of organic matrix composites is still not well understood. It is a very complex problem, depending on variables which are interrelated. Even the methods of studying the interface are greatly varied and complex. In this report alone, 14 different methods used to study aspects of the interface are reviewed. As the number of different analyses needed increases, it becomes progressively difficult for any one person to be an expert. Hence, communication among a group of specialists is crucial to begin to solve the problems of interfacial adhesion. Correlation between results of one test and another is indispensable for accurate interpretation. It is not even clear that all the necessary tests needed are available. For example, how do we observe liquid polymer conformation in relation to the orientation of graphite planes?

Besides complexity, definition of the problem is another reason that the interface is not fully understood. What is good adhesion? Even assessing the degree of adhesion quantitatively is not yet perfected. No single test has been devised which yields the actual interfacial shear strength. However, this quandary is typical of composite properties.

Some facts about organic matrix/graphite fiber composite interfaces are well established. First, interfacial adhesion greatly effects the composite. Adhesion can change its failure mechanism and mechanical and physical properties. However, typical models to predict properties do not adequately consider the effects of interfacial adhesion. Novel concepts such as molecular conformation may have to be incorporated in the models.

Second, adhesion is greater to high strength fibers than to high modulus fibers. This is essentially because adhesion is governed by fiber surface reactive sites. High strength fibers, because they are more imperfect, have more active sites than high modulus fibers. Additional functionality can be introduced by sizings and surface treatments. Bonding is increased primarily in two ways: (1) acid/base attractions, and (2) covalent bonding. Acid/base attractions are critical especially for adequate wetting, but also may be a technique to increase interfacial bonding. Covalent bonding is the strongest method of adhesion and may also reduce absorption of contaminants into the interface. Although sizings have proven to be adequate to induce adhesion with epoxy matrices, surface treatments, particularly plasmas, are an essential step for thermoplastic materials. Plasmas can induce covalent bonding and can be tailored to create the degree of adhesion required for the application. Carefully selected and controlled plasma treatments are the future for increasing adhesion in composite materials. Unfortunately, there appears to be a maximum to the functionality which can be introduced onto the fiber surface which cannot be exceeded by current methods. This indicates that either new fibers will have to be developed, or the basal planes of graphite fibers will have to be attacked to create imperfections. This process may degrade the mechanical properties of the fiber.

Third, graphite sticks better to epoxies than to thermoplastics. This indicates that to maximize adhesion, the matrix material must also have active sites. Sizings may help via interdiffusion. For semicrystalline polymers, transcrystallinity may help offset this effect. However, trying to solve adhesion problems without knowledge of the resin chemistry is preposterous. Either resin manufacturers will have to perform all of the research on adhesion, or they must put aside the notion of proprietary resins to allow academicians to do the work.

What is painfully obvious is that the past approach of trial-and-error to improve interfacial adhesion is not efficient as the number of fibers and matrix materials multiplies. The problem of increasing adhesion is solvable, but empiricisms are not satisfactory. Engineers need models to predict the properties of new systems that will allow them to grasp the important variables which will improve adhesion. Only scientific understanding of the chemistry and morphology of the resin and fiber will produce models of adhesion which will predict the effects of the interface on composite properties.

## References

1. W. D. Bascom and L. T. Drzal, *NASA Contractor Report 4084*, (1987).
2. W. Gutowski, *Interfaces in Polymer, Ceramic and Metal Matrix Composites: Proceedings of the Second International Conference on Composite Interfaces (ICCI-II)*, Hatsuo Ishida, ed. (Cleveland, Ohio: June 13-17, 1988), p. 735.
3. Elizabeth Berger, *Advanced Composites III, Expanding the Technology*, Proceedings of the Third Annual Conference on Advanced Composites, ASM International and Engineering Society of Detroit, sponsors. (Detroit, Michigan: Sept. 15-17, 1987), p. 309.
4. Willard D. Bascom, *NASA Contractor Report 178306*, (1987).
5. A. Crasto, S.-H. Own, and R. V. Subramanian, *Composite Interfaces: Proceedings of the First International Conference on Composite Interfaces (ICCI-I)*, Hatsuo Ishida and Jack L. Koenig, ed. (Cleveland, Ohio: May 27-30, 1986), p. 133.
6. P. Denison, F. R. Jones, and J. F. Watts, ICCI-II, p. 77.
7. T. F. Cooke, *Journal of Polymer Engineering*, 3 (7) (1987), p. 197.
8. J. Harvey, C. Kozlowski, and P. M. A. Sherwood, *Journal of Materials Science*, 22 (1987), p. 1585.
9. Dr. Ronald Allred, PDA Engineering, Albuquerque, New Mexico, private conversations.
10. John Delmonte, "Technology of Carbon and Graphite Fiber Composites," Van Nostrand Reinhold Company, New York. 1981, pp. 60 & 64.
11. L. T. Drzal, M. J. Rich, and M. F. Koenig, *Journal of Adhesion*, 18 (1985) p. 49.
12. N. B. Colthup, L. H. Daly, and S. E. Wiberly, "Introduction to Infrared and Raman Spectroscopy," Academic Press, New York and London. 1964, pp. 27-34.
13. S. Patel, G. Hadziloannou, and M. Tirrell, ICCI-I, p. 194.
14. P. Denison, et al., *Journal of Materials Science*, 23 (1988) p. 2153.
15. A. Ishitani, H. Ishida, G. Katagiri, and S. Tomita, ICCI-I, p. 195.
16. P. Denison, et al., ICCI-II, p. 239.
17. G. Dorey and J. Harvey, ICCI-II, p. 693.
18. T. Takahagi and A. Ishitani, *CARBON* 26 (1988), p. 392.
19. S. C. Bennett, PhD thesis, University of Leeds, 1976.
20. Eugene P. Bertin, "Principles and Practice of X-Ray Spectrometric Analysis," Plenum Press, New York-London. 1970, pp. 22-23, 60-61, and 596-600.
21. J. E. Castle and J. F. Watts, ICCI-II, p. 57.
22. Da Youxian, et al., *Composite Science and Technology*, 30 (1987) p. 119.
23. J. A. Peacock, et al., ICCI-I, p. 143.
24. J. B. Donnet, et al., ICCI-II, p. 35.
25. J. A. Peacock, et al., ICCI-I, p. 299.
26. Donald E. Adams, *Journal of Reinforced Plastics and Composites*, 6, p. 66.
27. Barbra L. Gabriel, "SEM: A User's manual for Materials Science," American Society for Metals, Metals Park, Ohio. 1985, pp. 17 & 66.
28. L. T. Drzal, M. J. Rich, and S. Subramoney, *Advanced Composites III*, p. 305.
29. P. S. Tehocaris, ICCI-I, p. 329.
30. M. Kryszewski and J. K. Jeszka, ICCI-I, p. 81.
31. M. R. Piggott and S. R. Dai, ICCI-II, p. 481.
32. M. R. Piggott, ICCI-I, p. 109.
33. H. Jahankham, and C. Gallotis, ICCI-II, p. 107.
34. W. D. Bascom and R. M. Jensen, *Journal of Adhesion*, 19 (1986) p. 219.
35. J. M. Whitney and L. T. Drzal, *Special Technical Publication 937, ASTM*, (1987) p.

36. T. Gendron, M. Waterbury, and L. T. Drzal, *Final Technical Report of Contract No. N00014-86-K-0393, Office of Naval Research*, (1987).
37. A. T. DiBenedetto, et al., ICCI-I, p. 47.
38. R. Stone, *Interim Technical Report of Contract No. 733615-86-C-5008, Air Force Wright Aeronautical Laboratories, Materials Laboratory*, (Oct 1988).